AIAA SciTech Forum
January 3-7, 2022, San Diego, CA & Virtual
AIAA SCITECH 2022 Forum

10.2514/6.2022-2486

Effect of Structural Modifications on Vibratory Response of a Panel under Ramp-Induced Shock / Boundary Layer Interaction

Marc A. Eitner[1] and Yoo-Jin Ahn[2] and Mustafa N. Musta[3] and Noel T. Clemens[4] and Jayant Sirohi[5]
The University of Texas at Austin, Austin, TX, 78712, USA

The vibration of a compliant panel under a shock / boundary layer interaction (SBLI) induced by a compression ramp in a Mach 2 flow, is investigated experimentally. The panel is made from brass shim stock of length (streamwise), width (spanwise) and thickness of 122 mm by 63.5 mm by 0.25 mm, respectively. The 20° compression ramp is placed near the downstream edge of the compliant panel, and it creates a shock-induced turbulent separated flow that extends over the downstream 20% of the panel. Large pressure fluctuations occur in the region of the separation shock foot unsteadiness. The pressure fluctuations increase vibration amplitudes of the higher panel modes, especially the second mode, which has an antinode near the shock foot region. In this work, the authors use structural modifications of the baseline compliant panel to mitigate vibrations induced by the large pressure fluctuations of the shock foot unsteadiness. A thin rib is attached in the spanwise direction to the lee side of the panel at the location of SBLI. In one configuration, the rib is attached to the panel using epoxy adhesive, which creates a stiff connection. In another configuration, the rib is attached to the panel via double-sided viscoelastic tape, which adds significant damping to the system. The panel vibration and surface pressure field are measured using stereoscopic digital image correlation and pressure sensitive paint. Results show that especially the second vibration mode of the panel is reduced through the addition of the rib. This effect is more pronounced in the case where the viscoelastic tape was used, where a 72% reduction in vibration is observed.

I. Nomenclature

h	=	panel thickness
L	=	free panel length
W	=	free panel width
x	=	stream-wise coordinate
y	=	transverse coordinate
w	=	out-of-plane panel deformation

[1] Postdoc, AIAA member
[2] Graduate student, AIAA member
[3] Lecturer, AIAA member
[4] Professor, AIAA fellow
[5] Professor, AIAA associate fellow

II. Introduction

Supersonic flight vehicle design is a highly multidisciplinary process and needs to account for interactions between thermal, aerodynamic and structural loads. The structural design of the outer mold line is driven by lightweight constraints and thus results in fairly compliant structures. Because of this, adverse flow-structure interactions can occur more easily and lead to failures such as high-cycle fatigue.

A typical occurrence of these unwanted interactions occurs upstream of geometric disturbances (such as fins or control surfaces), where shocks interact with turbulent boundary layers. These shock / boundary layer interactions (SBLI) can lead to unsteady boundary layer separation that is associated with intense fluctuating pressure loads that are much larger than those induced by the turbulent boundary layer alone. While this interaction is already quite complex and is still challenging for state-of-the-art CFD, the problem becomes even more difficult when structural compliance is relevant. Structural vibrations are influenced by the surface pressure field and in turn can influence the flow field, which leads to a coupling between flow and structure.

A significant amount of experimental and numerical research has been performed in recent years that investigates the complex fluid-structure interactions of SBLI in the presence of compliant structures. Within the last two years alone, multiple papers have been published on that topic, a few of them are summarized in the following.
Varigonda et al. published several studies [1], [2] that utilized pressure sensitive paint (PSP) and discrete strain measurements from piezo-electric sensors to investigate FSI at different Mach numbers and structural forcing conditions. Tan et al. [3] used discrete pressure transducers, Schlieren imaging and oil flow visualization to investigate especially the effect of static panel curvature on the flow field. They achieved different curvatures by varying a compressive strain in the panel and showed that larger curvatures lead to shorter separation lengths. Spottswood et al. [4] published the findings of a multiyear experimental campaign on the FSI of a steel panel, using a variety of discrete and full-field measurement techniques. They incorporated the effect of heated flow in their measurements and found an interesting bifurcation of the vibrational behavior. Neet et al. [5] performed test in a Mach 4 Ludwid tube and similarly to [3] investigated the effect of static panel curvature on the flow field using Schlieren imaging. Schöneich et al. investigated ramp-induces SBLI in the case where a compliant panel was embedded in the ramp. They performed experiments at varying ramp angles and used infrared cameras to measure the temperature field. A study by Tripathi et al [6] investigated the effect of panel back pressure on the flow field and found significant changes in separation length when the cavity pressure was reduced. Experimental studies such as [7] [8] used the setup to develop experimental camera-based techniques to better investigate such systems. Most of the research is fundamental in nature and aims to better understand the dynamic behavior of such coupled systems. The investigated systems are almost exclusively thin, rectangular panels. This paper goes a step further and explores experimentally how the dynamics of such a system change when structural modifications are made to the panel.

Modifying a structure to optimize the vibratory behavior of coupled fluid-structure systems is commonly referred to as aeroelastic tailoring. Several ways have been explored in past research studies that aim to reduce panel vibration in the presence of flow, using either passive or active components. Abdel et al. [9] added thin piezo-electric actuators to the panel to create surface strains that successfully counteracted the panel vibrations for an aeroelastic instability known as panel flutter. Yang et al. [10] added a viscoelastic layer to a composite panel to increase structural damping and thus increase the critical dynamic pressure at which panel flutter occurs. Marques et al. [11] used an aeroelastic computer model and a genetic algorithm to modify the fiber orientation and the laminate density of a composite panel to also increase the critical dynamic pressure. Such an approach is powerful but only possible if an adequate model of the system is available. For the case of SBLI over a compliant panel, no such model exists and thus this approach is not possible.
The lack of a numerical model means that no large parameter space can be explored and thus no optimal structural modification can be found. The approach taken in this work is to make engineering judgements based on available experimental results and theory to create, and experimentally test, a few specific modifications to the baseline panel. The previous experimental results stem from the literature as well as a recently completed test campaign [12]. In that test campaign, a thin rectangular brass panel (length L=122.0 mm, width W=63.5 mm, thickness h=0.254 mm) was inserted into the floor of a Mach 2 wind tunnel just upstream of a 20° compression ramp and simultaneous measurements of the deformation and surface pressure fields were made. This paper extends upon that test campaign by attaching a small rib to the lower side of the panel, to modify the flow-induced vibration. The design and location of the panel is guided by experimentally measured mode shapes and surface pressure distributions.

III. EXPERIMENTAL SETUP

All experiments were performed in the Mach 2 blow-down wind tunnel, located at The University of Texas at Austin. A schematic of the full experimental setup is shown in Figure 1. Two high-speed monochromatic cameras (Vision Research Phantom Miro M310) are setup below the tunnel and view the panel through a sealed enclosure with a window at the bottom. These cameras record the transient panel deformation by tracking a speckle pattern on the panel using stereoscopic digital image correlation (3D-DIC). The flow-facing side of the panel is painted with fast reacting pressure sensitive paint (PSP). A high-speed camera (Mini Fastcam AX50) located above the tunnel images the painted surface through a viewing window in the ceiling of the tunnel test section.

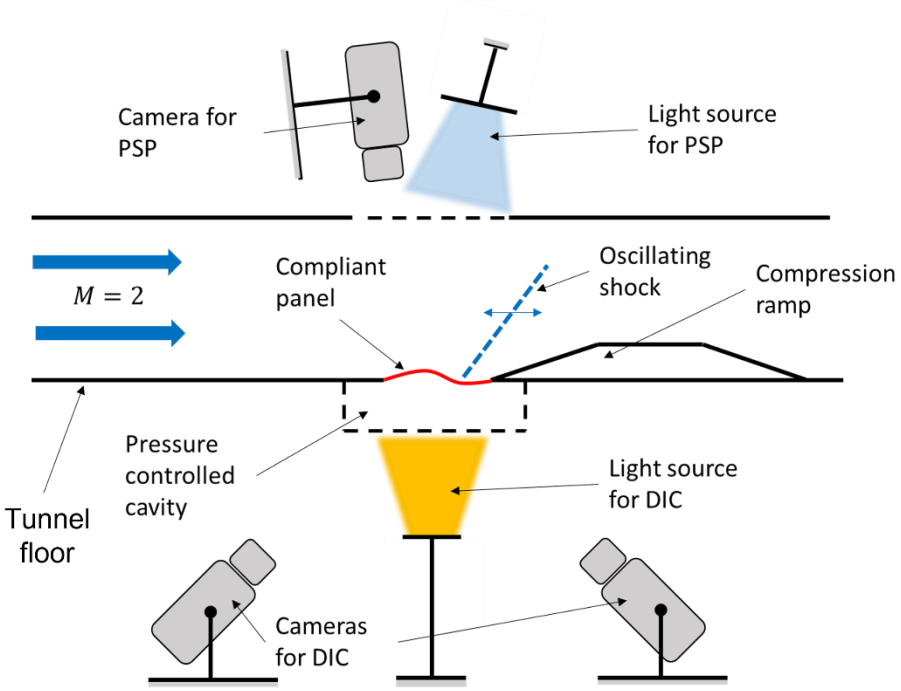

Figure 1: Full experimental setup

The panel is cut from brass shim stock (260 brass) and is bonded to a brass base using an epoxy resin (EA E-60 HP by LOCTITE). These two parts connected form an insert which is bolted into the floor of the tunnel test section, such that the panel is flush with the tunnel floor. This is shown in Figure 2. The lower side (lee side) of the panel is enclosed with a pressure-controlled box, forming a cavity below the panel. A vacuum pump and pressure transducer are connected to the cavity, allowing control of its pressure. During the tunnel run the static pressure in the test section drops to about 44 kPa (6.4 psia) and thus the pressure in the cavity is also reduced to avoid a large static deformation of the panel.

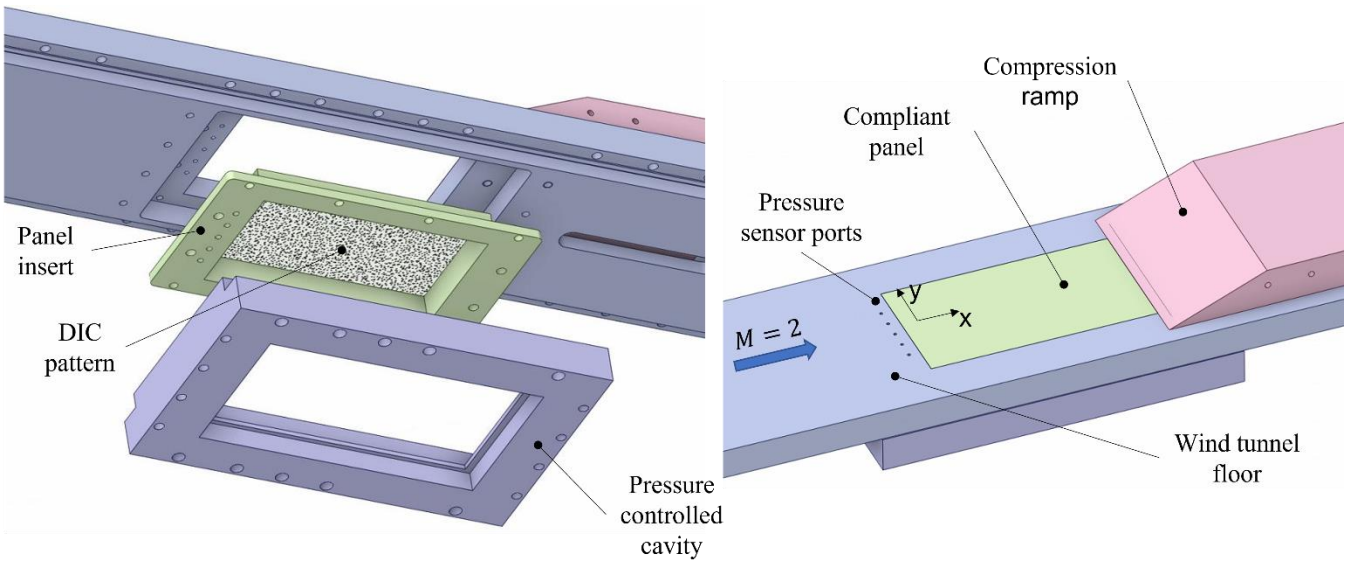

Figure 2: Panel installation in floor of wind tunnel test section

A. Digital Image Correlation

The lower side of the panel was equipped with a adhesive label onto which a speckle pattern was printed. This pattern was custom designed for the specific camera setup, choice of lenses and resolution. The python code "speckle pattern.py" from the Laboratory for Dynamics of Machines and Structures at the University of Ljubljana, Croatia, was used for this task. Preliminary tests revealed that the addition of the DIC sticker does not modify the natural frequencies of the panel. Vibration of the camera setup was measured below 100 Hz and was subsequently filtered out during post-processing of the deformation time-histories. The software Davis 10 by LaVision was used for calibration and computation of the deformation fields. A facet size of 27×27px with an overlap of 9px was used for the computation. A noise floor was established by measuring the deformation in 100 still images, resulting in a standard deviation below $4\mu m$ for each facet.

B. Pressure Sensitive Paint

A polymer-ceramic pressure sensitive paint was mixed on location and sprayed onto the panel using a spray gun (Paasche Airbrush H0318). The paint consisted of a silicone binder, to which TiO_2 particles were added as well as the luminophore rhutenium. The applied paint layer was very thin (20-40μm) and impact tests showed that the PSP did not affect the panel dynamics. The paint was calibrated dynamically on a rigid panel with several holes for pressure transducers (KULITE XCQ-062), that were mounted flush with the surface. By comparing power spectra of surface pressure measurements from the Kulite transducer as well as an average of the nearby pixel intensities (surface pressure is related to intensity with PSP) it was shown that the fast response follows the true pressure spectrum well above 10kHz.

IV. Supersonic flow environment

The supersonic flow enters the test section at a Mach number of $M_\infty = 2$ and with a turbulent boundary layer (BL) height of approximately $\delta_{99} = 12.5$ mm. The 20° compression ramp induces a shock-induced turbulent separated flow, with a separation length-scale that is about $2\delta_{99}$ upstream of the ramp corner. Downstream of the BL separation the mean surface pressure increases due to the compression process induced by the ramp. The mean and standard deviation of the surface pressure field obtained from a test with a rigid panel are shown in Figure 3 (a) and (b), respectively. The upstream edge of the SBLI coincides with a region of large pressure fluctuation, which is caused by separation shock-foot unsteadiness. The shock foot is the location where the separation shock meets the floor of the wind tunnel. The seven small circles along the centerline are holes for pressure transducers that were used to calibrate the PSP.

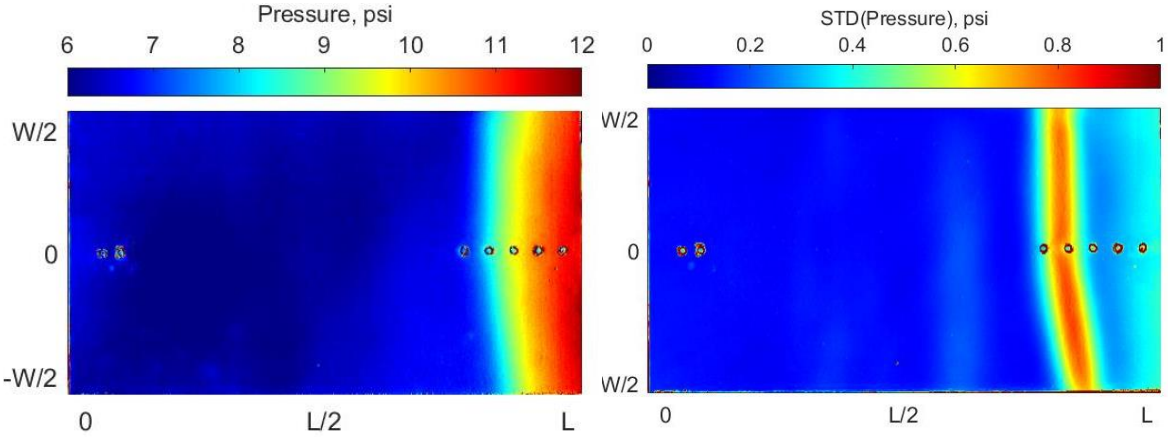

Figure 3: Surface pressure over rigid panel, (a) mean and (b) standard deviation; flow from left to right

V. Structural Modifications

The region under the shock foot is a significant source of excitation for the panel since the frequency band of shock-foot unsteadiness is broadband and overlaps with the vibrational modes of the panel. The location of peak standard deviation is located about 80% of the panel length and forces especially the second structural mode since it is close to the antinode of that mode. This is known from a previous test campaign [12]. It was also observed that the location of SBLI is hardly affected by the compliance of the panel. This means that the structure is locally excited, a fact that can be exploited for vibration mitigation. By making a small structural modification to the panel, the effect of the local forcing function can be significantly reduced. This paper demonstrates the effect of attaching a small rib to the panel at the location of the peak pressure fluctuation. The rib consists of the same material as the panel (brass shim) and is of dimension 10 mm× 25.4 mm×0.79 mm. The weight is 10% of the plain panel weight. An image of the panel insert with the attached rib (highlighted by red rectangle) is shown in Figure 4, along with relevant dimensions.

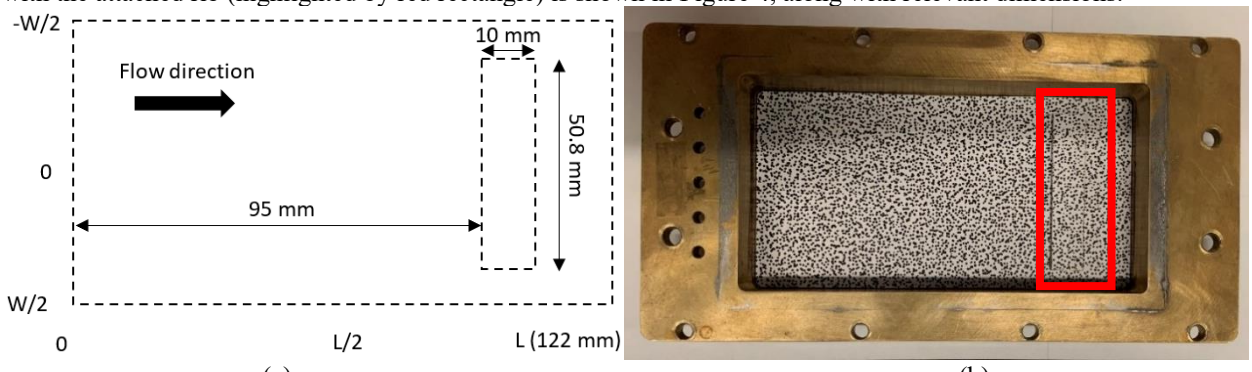

Figure 4: Panel insert with attached rib. (a) schematic, (b) image of panel insert with rib and speckle pattern for DIC

The panel is tested in three different configurations. First, the baseline (plain) panel in its unmodified state is tested. Then the rib is attached to the panel via double sided, viscoelastic tape (3M VHB, 0.6 mm thick). This configuration increases the mass and damping but does not increase the stiffness of the panel, due to the low shear modulus of the tape. After the tests on the taped configuration were completed, the rib and tape were detached from the panel. Then the rib was reattached to the panel using high-strength two component epoxy (EA E-60HP by LOCTITE). In this configuration the rib adds stiffness (as well as mass) to the panel due to the high shear stiffness of the adhesive bond layer.

In the taped configuration the damping increase is due to an effect known as constrained layer damping. This effect is demonstrated here with a simple free vibration cantilever beam experiment shown in Figure 5. A brass beam of same width and thickness but only half the length is attached to a cantilever beam using double sided, viscoelastic tape. The bending deformation of the cantilever beam induces large strain in the left side of the tape (facing the long cantilever beam). Due to the low shear stiffness of the tape, the short, attached beam on the right is mostly unstrained. Thus, the tape exhibits large shear strain during vibration of the cantilever beam. A large amount of vibrational energy is dissipated in the tape due to this shear strain. For example, the damping ratio of the fundamental beam bending mode was increased from 0.29% to 9.57% through this process.

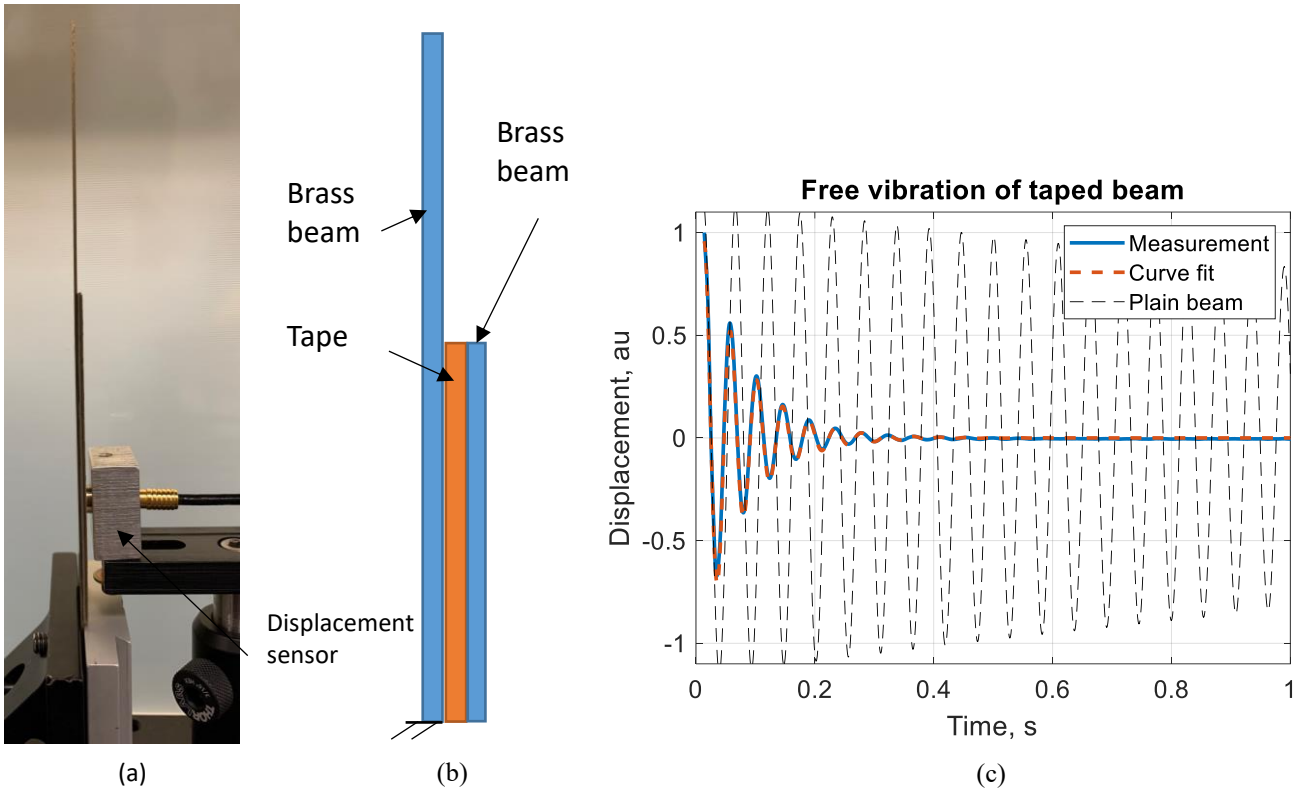

(a) (b) (c)

Figure 5: Experimental setup (constrained layer damping) and results to show effect of viscoelastic tape on damping. (a) image of beam with sensor, (b) schematic of setup, (c) free vibration time-histories of beam without ('plain') and with ('measurement') constrained layer damping.

VI. Experimental modal analysis

The natural frequencies of each panel configuration were obtained experimentally from impact testing in the absence of flow. Each panel was tested when installed in the wind tunnel floor with the cavity box attached. The three panel configurations are denoted as:

- **Plain:** The panel without any rib attached (baseline configuration).
- **Taped rib:** The rib was taped to the panel (using double sided viscoelastic tape).
- **Fixed rib:** The rib was attached to the panel using two-component epoxy

The impact tests were performed using a capacitive displacement sensor (Microepsilon capaNCDT 6110 CS05) and a small metal tip impact hammer. The frequency response functions were computed from five averaged impacts and the peak picking method was utilized to obtain the natural frequencies. The resulting frequencies of the first two modes are listed in Table 1.

Table 1: Natural frequencies of panel from impact tests

Plain panel		Taped rib		Fixed rib	
Mode 1	Mode 2	Mode 1	Mode 2	Mode 1	Mode 2
383 Hz	453 Hz	433 Hz	Not identified	395 Hz	506 Hz

Note that in both cases with the rib the natural frequencies increase. In the case of the fixed rib, the added stiffness outweighs the added mass and thus the natural frequency increases. In the case of the taped rib, added mass alone leads to a slight change in fundamental mode shape; the effective length of the first mode vibration is decreased and thus results in an increase in frequency. This effect was qualitatively shown through a finite element analysis, which is omitted here for brevity. In the case of the taped rib, the vibration amplitudes of the second mode were so small that no clear modal identification could be performed, already indicating that the panel modification performed well.

VII. Panel vibration with flow

This section characterizes the flow-induced vibration of the panel, obtained from DIC. To get an idea of the overall vibration, the standard deviation of each point on the panel is computed and plotted as a single image. This allows to visualize and quantify the vibrational energy of each panel. These images are dominated by the deformation of the fundamental panel mode, which carries the most vibrational energy in the structure. Shown in Figure 6 are the plots of the standard deviation as well as the mean deformation for a test performed on the baseline panel (without a rib). The vibration amplitude is largest near the panel center and the distribution looks symmetric about the panel center. Compared to the case with the rib, shown in Figure 7 and Figure 8, it is immediately noticeable that by attaching the rib in either configuration, the overall vibration of the panel is reduced by about 25%. The peak vibration of the taped and fixed rib configurations are fairly similar but the overall vibration energy is larger for the fixed rib panel, since the vibration extends over a larger area. This can be seen by comparing Figure 7 (a) with Figure 8 (a) near the rib region.

The mean of the deformation w shows that the panel is deformed downwards (into the cavity) especially near the downstream end. This follows from the high-pressure region associated with the SBLI, as is shown in Figure 3 (a). The mean deformation of the panel depends mostly on the cavity pressure, which varied slightly, due to air leaks. A large mean deformation can affect the stress in the panel and thus also modify the overall vibration and natural frequencies. However, in a separate analysis (not shown here for brevity) it was determined that the mean deformation induced by the cavity pressure played only a secondary role in the panel vibration. This was determined by comparing the vibrations of the panel with the fixed rib in three test runs with varying cavity pressure. The mean deformation looked vastly different, but the mode shapes and vibrational energy looked mostly the same, only the natural frequencies were increased.

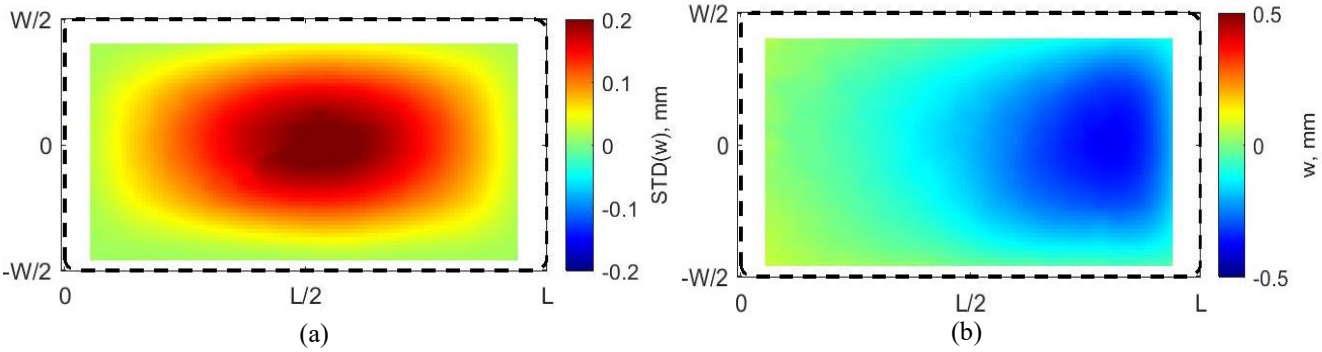

Figure 6: Baseline (plain) panel, (a) standard deviation and (b) mean of deformation

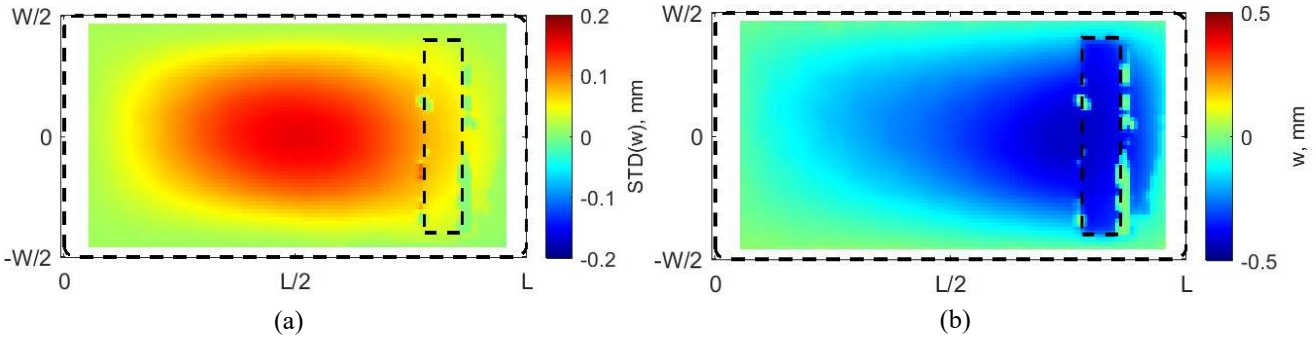

Figure 7: Panel with taped rib, (a) standard deviation and (b) mean of deformation. Small, dashed rectangle shows location of rib.

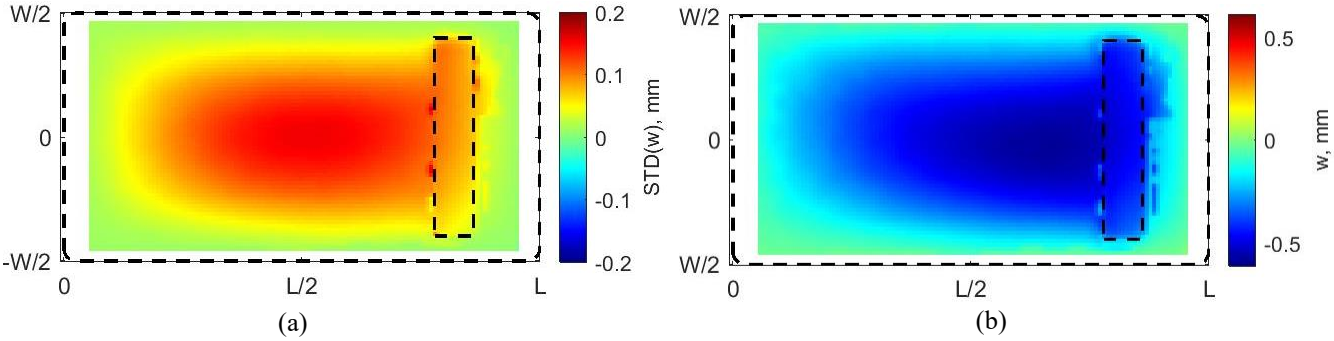

Figure 8: Panel with fixed rib, (a) standard deviation and (b) mean of deformation. Small, dashed rectangle shows location of rib.

Comparison of power spectra

The full-field plots shown above demonstrate the spatial distribution of energy in the panel but lack information about the frequency content. Analysis of deformation power spectra at single locations on the panel show that multiple modes participate in the overall panel vibration. However, a slight change in mode shapes between the different configurations will have large effects on the power spectra and thus comparison at a single location becomes difficult. An alternative way of comparing power spectra from different panel configurations is proposed here, which is independent of the location on the panel. The method is based on the mode indicator function employed by Brinker and Anderson [13]. First, the cross-power spectral density matrix $[G_{yy}(\omega_i)]$ is computed for all channels of the measurement matrix. The matrix is of dimension $m \times m$, where m is the number of measurement channels. In this case m is equivalent to the number of DIC facets at which deformation data was obtained. The matrix is computed for each frequency bin ω_i, where the amount of frequency bins is determined by the FFT, window size and overlap used to compute the cross power spectral density. Next, the singular value decomposition of the matrix $[G_{yy}(\omega_i)]$ is computed as:

$$[U_i, S_i, V_i] = svd[G_{yy}(\omega_i)] \qquad (1)$$

The subscript i denotes a specific frequency bin, meaning that this singular value decomposition is performed at each frequency bin. The dominant information of the system is contained in the first (highest) singular value. By plotting the first singular value $S_i[1,1]$ for all frequency bins one obtains a deformation power spectrum of the system that is not based on a single location, but rather on energy. It is therefore a suitable way of comparing power spectra between different panel configurations.

Figure 9 shows the deformation power spectra for the three different panel configurations (plain, taped, fixed), computed using the above-described method. In addition, the POD mode shapes for the baseline panel case are shown. They are obtained from a regular POD analysis of the measured deformation data. Since the POD modes of a structural system are very similar to its structural mode shapes, they have a single dominant frequency component and can thus be associated with peaks in the power spectrum. This association is shown in Figure 9 through arrows between the POD mode shapes and the power spectrum peaks.

The spectrum for the baseline panel (without a rib) shows multiple peaks, indicating structural modes, whose amplitudes decrease with frequency, as is typical for a structural system subjected to broad-band excitation. In the two

cases where the rib is attached, the system is still dominated by the fundamental mode (at around 500 Hz). From the analysis of the vibrational energy in the previous section (standard deviation of deformation) it is known that the peak vibration amplitude in the two cases with attached rib are approximately equal to each other and about half of the plain panel case. Comparison of the peaks of the fundamental mode in the power spectra in Figure 9 shows that the taped panel peak is clearly below the fixed panel peak. This stems likely from the fact that while the vibration amplitudes are similar, less area of the panel vibrates in the taped configuration as compared to the fixed rib configuration. When looking at the second panel mode (at around 700 Hz) the peaks of the cases with rib are almost an order of magnitude below the peak of the plain panel case. This indicates that the rib decreased the vibration amplitude of the second mode. A similar trend is observed for higher modes as well.

Note that the peaks associated with the natural frequencies of the panel configurations are at much higher frequencies than those measured from the impact tests without flow. The two major reasons for frequency increase are in-plane stresses and fluid-structure coupling. In-plane stresses arise from out-of-plane static panel deformation (due to pressure differences in free-stream, cavity, and separation bubble) and thermal contraction (due to flow-induced cooling of the panel). Fluid-structure coupling in the case of a rectangular plate occurs when the panel vibration is large enough to disturb the boundary layer and modify the surface pressure. This process can be modeled by including a so-called aerodynamic stiffness matrix into the equation of motion. The SBLI and cooling of the panel need to be considered for a detailed model. This is because the aerodynamic stiffening effect is no longer present in the separated flow region downstream of the shock interaction and the size of the flow separation region is unsteady. The shock-induced turbulence further increases the local heat transfer and results in thermal gradients in the panel, which in turn greatly affect the panel stiffness. To the best knowledge of the authors no aerodynamic stiffness matrix has been derived, which includes an SBLI. Furthermore, the lack of thermal measurements (such as with temperature sensitive paint) makes it difficult to quantify the stiffening effect from thermal gradients. Because of these reasons, no attempt at any simplified modeling of the coupled flow-structure interaction was made.

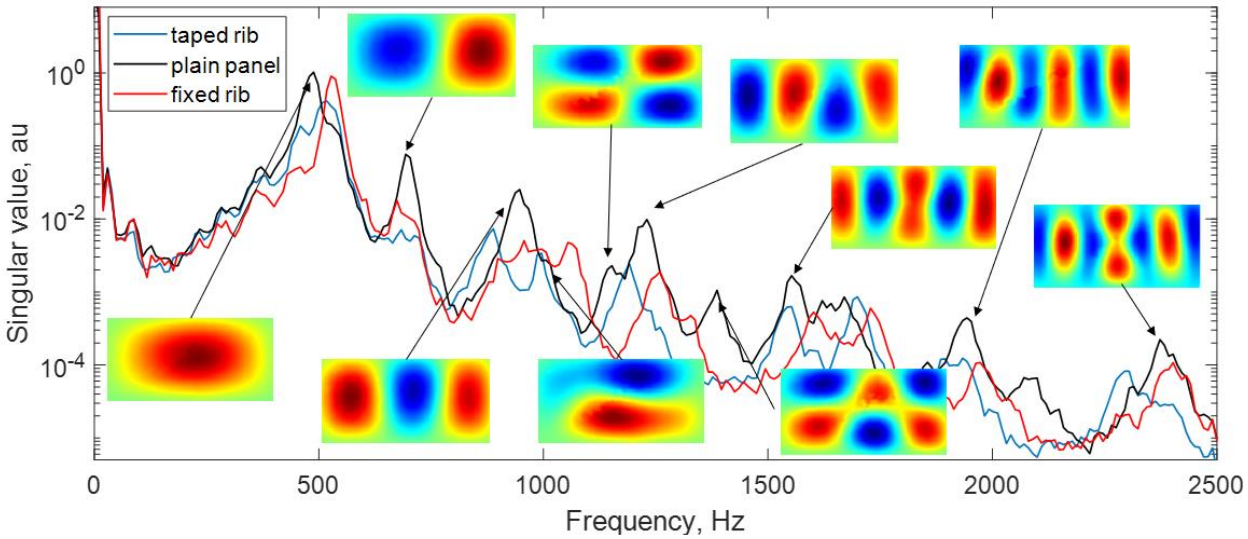

Figure 9: Comparison of power spectra from 1st singular value of cross-power spectral density matrix, along with POD mode shapes of plain panel

POD mode shapes and Energy

The analysis above shows that the vibration of the panel is dominated by the fundamental mode. In this section the vibration is decomposed into modal components. Proper Orthogonal Decomposition (POD) is employed to obtain vibration modes of the system from the measured deformation. Shown in Figure 10 (a) are the fundamental POD mode shapes of each panel configuration. The deformation data was first high-pass filtered (3^{rd} order Butterworth filter, cutoff frequency 100Hz) to get rid of spurious motion induced by camera shaking. The natural frequency of each mode can be clearly identified from the temporal coefficients/time histories associated with each mode. After the natural frequency was calculated, an estimate was made of the energy in the mode. This was done by first band-pass filtering the vibration data (40 Hz bandwidth, 7^{th} order Butterworth filter) centered around the natural frequency. From

the resulting filtered data, the temporal standard deviation was computed at each point on the panel and surface plots were created. These plots are shown in Figure 10 (b). The standard deviation plots look similar to those shown in Figure 6 (a), since the majority of the vibrational energy is contained in the fundamental mode. As expected, there is good spatial agreement between the mode shapes and the band-pass filtered standard deviation plots.

The same analysis is performed for the second mode and the resulting plots are shown in Figure 11. The second mode for the plain panel is skewed in the downstream direction. This is due to the flow-structure coupling between panel vibration and the supersonic flow upstream of the shock interaction and has been observed in previous experiments as well [12]. The standard deviation plots in Fig. 11(b) show a large decrease in the second mode vibrational energy when the rib is attached. This is especially true for the taped rib configuration where the maximum standard deviation is reduced by 72% compared to the baseline (plain) panel. This furhter confirms the analysis of the mode indicator functions shown in Figure 9.

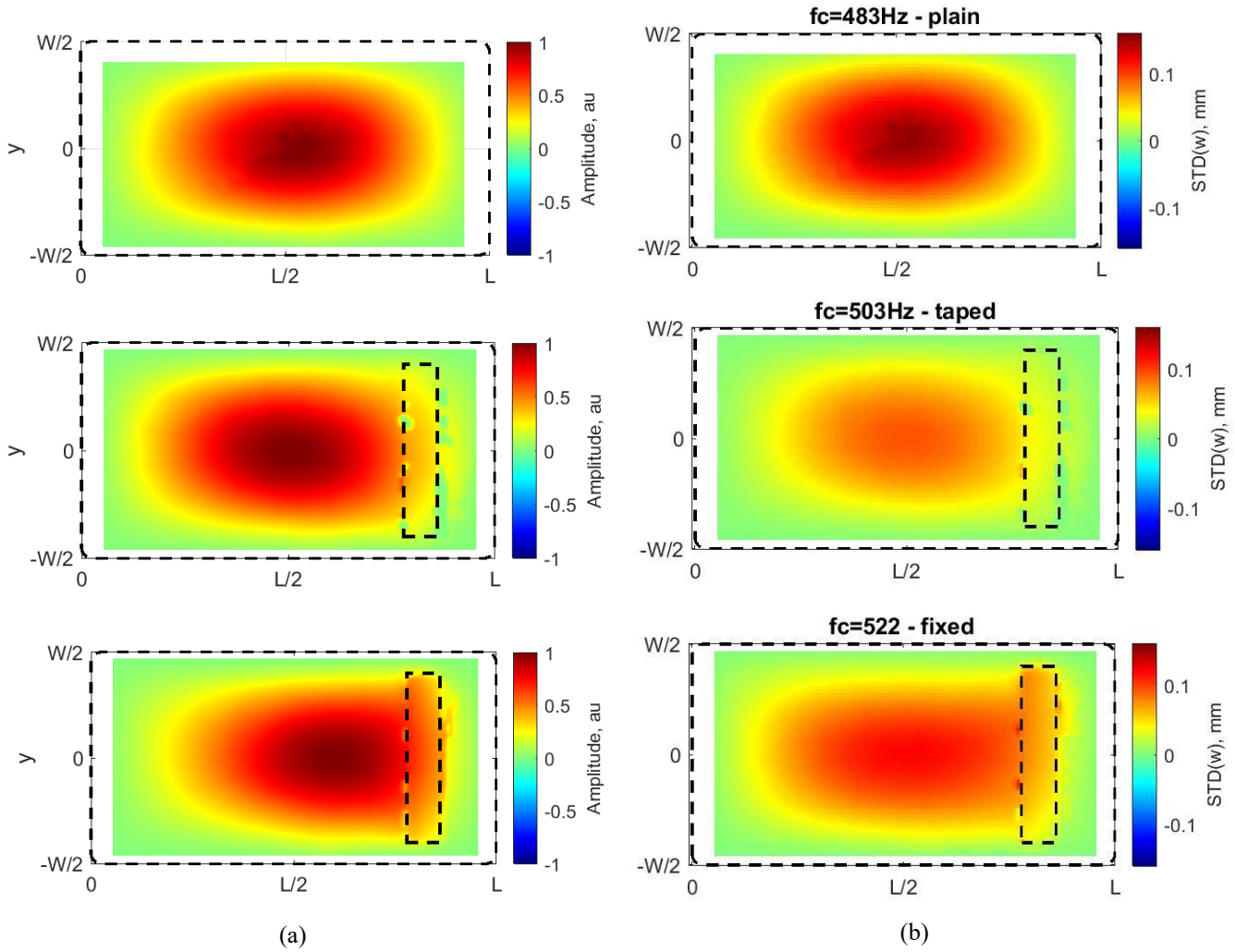

Figure 10: Fundamental panel mode, (a) mode shape from POD and (b) standard deviation of band-pass filtered deformation

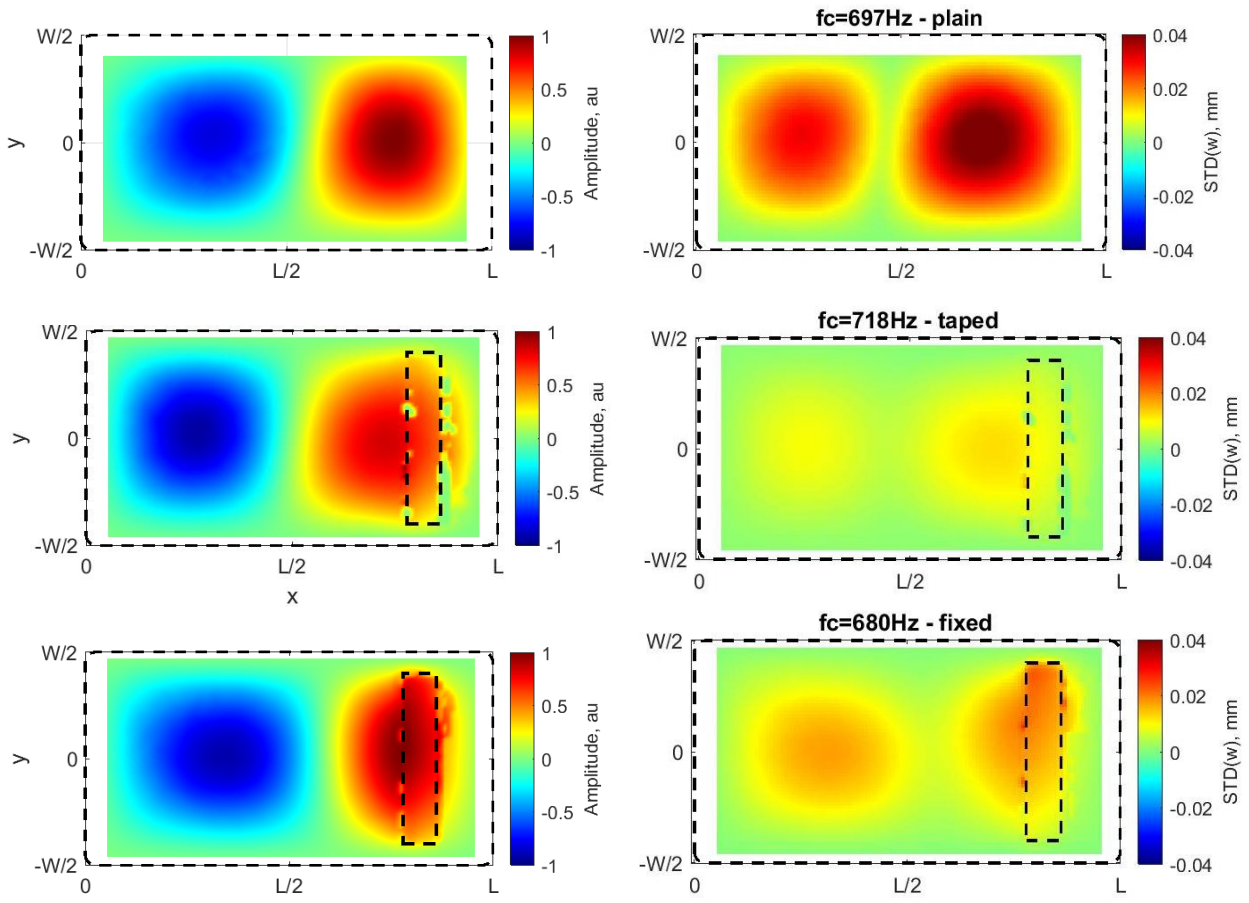

(a) (b)

Figure 11: Second panel mode, (a) mode shape from POD and (b) standard deviation of band-pass filtered deformation

VIII. CONCLUSION

The results presented in this paper show that the vibration of a coupled fluid-structure system can be greatly reduced through localized structural modifications. A rectangular panel, located upstream of a compression ramp induced SBLI, was forced by the fluctuating pressure field associated with separation shock foot unsteadiness. By adding a rib to the panel, the overall vibration was reduced, especially the vibration of the second mode. The rib was attached at the location where the forcing occurs, which coincides with the antinode of the second structural mode. The configuration in which the rib was attached to the panel with double sided, highly viscoelastic tape was very effective at vibration reduction. This configuration increased the damping of the system through constrained layer damping but added no additional stiffness to the panel. On the contrary, the configuration where the rib was directly attached to the panel using epoxy adhesive increased the stiffness but was less effective at vibration reduction than the taped configuration. Neither configuration significantly modified the mode shapes of the panel compared to the plain configuration. Due to the lack of an available computer model, no large parameter space for the structural modifications (location, rib dimensions, …) could be investigated and thus no optimal solution was explored. Good results were still obtained (regarding vibration reduction) simply based on intuitive analysis of vibration modes. The results presented in this paper are therefore simply an initial exploration of the possibilities of employing aeroelastic tailoring in the presence of SBLI and provide an initial data set to be improved in future investigations.

IX. ACKNOWLEDGEMENTS

This work was supported by the National Science Foundation under award # 1913587. The authors would like to thank Jeremy Jagodzinski for assisting with the measurements.

X. References

[1] S. Varigonda and V. Narayanaswamy, "Investigation of Shock Wave Oscillations over a Flexible Panel in Supersonic Flows," AIAA paper 2021-0912, *AIAA Aviation Forum*, 2019.

[2] S. Varigonda, C. Jenquin and V. Narayanaswamy, "Impact of Panel Vibrations on the dynamic field properties in supersonic flow," AIAA paper 2021-2926, *AIAA Aviation Froum*, 2021.

[3] S. Tan, P. Bruce and M. Gramola, "Oblique Shockwave Boundary Layer Interaction on a Flexible Surface," AIAA paper 2019-0097, *AIAA Scitech Forum*, 2019.

[4] S. M. Spottswood, T. J. Beberniss, T. G. Eason, R. A. Perez, J. M. Donbar, D. A. Ehrhardt and Z. B. Riley, "Exploring theresponse of a thin, flexible panel to shock-turbulent boundary-layer interactions," *Journal of Sound and Vibration,* vol. 443, pp. 74-89, 2019.

[5] M. C. Neet and J. M. Austin, "Effects of Surface Compliance on Shock Boundary Layer Interaction in the Caltech Mach 4 Ludwieg Tube," AIAA paper 2020-0816, *AIAA Scitech Forum*, 2020.

[6] A. Tripathi, J. Gustavsson, K. Shoele and R. Kumar, "Response of a Compliant Panel to Shock Boundary Layer," AIAA paper 2021-0489, *AIAA Scitech Forum*, 2021.

[7] T. Beberniss and D. Ehrhardt, "Visible Light Refraction Effects on High-Speed Stereo Digital Image Correlation Measurement of a Thin Panel in Mach 2 Flow," *Experimental Techniques,* vol. 45, no. 3, pp. 241-255, 2021.

[8] M. Eitner, M. Musta, L. Vanstone, J. Sirohi and N. Clemens, "Modal parameter estimation of a compliant panel using phase-based motion magnification and stereoscopic digital image correlation," *Experimental Techniques,* vol. 45, no. 3, pp. 287-296, 2020.

[9] K. Abdel-Motagaly, X. Guo, B. Duan and C. and Mei, "Active Control of Nonlinear Panel Flutter Under Yawed SupersonicFlow," *AIAA journal,* vol. 43, no. 3, pp. 671-680, 2005.

[10] X.-D. Yang, T.-J. Yu, W. Zhang, Y.-J. Qian and M.-H. Yao, "Damping effect on supersonic panel flutter of composite platewith viscoelastic mid-layer," *Composite Structures,* vol. 137, pp. 105-113, 2016.

[11] F. Marques, S. Natarajan and A. Ferreira, "Evolutionary-based aeroelastic tailoring of stiffened laminate composite panels insupersonic flow regime," *Composite Structures,* vol. 167, pp. 30-37, 2017.

[12] M. Eitner, Y. Ahn, M. Musta, L. Vanstone, J. Sirohi and N. Clemens, "Effect of Shock Wave Boundary Layer Interaction on VibratoryResponse of a Compliant Panel," AIAA paper 2021-2493, *AIAA Aviation Forum*, 2021.

[13] R. Brincker, L. Zhang and P. Andersen, "Modal identification from ambient responses using frequency domain decomposition," in *18th International Modal Analysis Conference IMAC*, San Antonio, TX, 2000.

[14] A. G. Schöneich, T. J. Whalen, S. J. Laurence, B. T. Sullivan, D. J. Bodony, M. Freydin, E. H. Dowell, L. J. Stacey and G. M. andBuck, "Fluid-Thermal-Structural Interactions in Ramp-Induced Shock-Wave Boundary-Layer Interactions at Mach 6," AIAA paper 2021-0912, *AIAA Scitech Forum*, 2021.